

Fabrication of 3D Graphene and 3D Graphene Oxide Devices for Sensing VOCs

So Matsuyama, Tomoaki Sugiyama, Toshiyuki Ikoma, and Jeffrey S. Cross
Department of Metallurgy and Ceramics Science, Tokyo Institute of Technology, 2-12-1
Ookayama, Meguro-ku, Tokyo 152-8550, Japan

ABSTRACT

Detection of volatile organic compounds (VOCs) emitted from cancerous tumor cells in exhaled human breath allows for early diagnosis of various types of cancers. 3D graphene with a large surface area is considered a suitable material for creating novel sensitive VOCs sensors. In this study, 3D graphene and 3D graphene oxide were synthesized from graphene oxide suspension, hydroquinone and formaldehyde by employing polymerization and reduction. The capability of VOC gas sensing was evaluated by measuring the electrical current response in flowing N₂ gas over a range of concentrations of acetone or 1-butanol at room temperature. It was observed that the device current correlated well with the VOC concentration. The adsorption of acetone decreased the current, but the adsorption of 1-butanol increased the current during sensing. 3D graphene oxide device was more sensitive than 3D graphene device because of the high concentration of oxygen-containing functional groups on the surface. These results indicated that 3D graphene and 3D graphene oxide may be the suitable materials for VOCs sensing devices.

INTRODUCTION

Graphene is two-dimensional (2D), one-atom-thick planar sheet with a honeycomb lattice composed of carbon atoms binding with sp² hybridized orbital. Numerous research studies have been carried out in the fields of electronics, batteries, and sensors [1] due to its superior electric conductivity and high specific surface area-to-volume ratio. In particular, the gas sensing based on graphene and its derivatives have been widely investigated [2]. The adsorption of gas molecules on the surfaces changes its electrical conductivity due to variation of the local carrier densities. The adsorbates can be electron donors or acceptors, resulting in detectable changes in electrical conductivity [3]. For example, NH₃, NO₂, acetone and ethanol were employed for sensing gases [4-5]. However, it is difficult to improve sensitivity due to the limitation of contact surface area of gas molecules on a single layer of graphene.

Three-dimensional (3D) graphene and its derivatives have been fabricated by a chemical vapor deposition method [6-7] and from graphene oxide (GO) as a precursor [8-10], since graphene has a limited surface area per a volume. 3D graphene has complex porous structures and high electric conductivities, of which properties are applicable for not only gas sensor, but also solar cells without Pt based electrodes [11]. The interconnected pores in the aerogel structure act as a diffusion path of gas molecules, which has been applicable for NO₂ gas sensing [12-13].

Volatile organic compounds (VOCs) emitted from the human body have been identified by ion flow tube mass spectrometry [14] and gas chromatography mass spectrometry [15]. There are approximately 250 VOCs in which some VOCs are related to specific carcinoma. Acetone and 1-butanol emitted from human breath are biomarker candidates. In this study, detection of low concentrations of acetone and 1-butanol as VOCs was investigated by using 3D graphene and 3D graphene oxide devices.

EXPERIMENT

Synthesis of 3D graphene oxide and 3D graphene

A 5 g/L graphene oxide suspension was purchased from Graphene laboratory Co. Ltd. 3D graphene oxide and 3D graphene were synthesized by employing polymerization or/and reduction as follows [16]. 61.2 mg of hydroquinone ($C_6H_6O_2$), 82.3 μ L of a 37wt% formaldehyde (CH_2O) and sodium carbonate (Na_2CO_3) as a catalysis were mixed into 5.0 mL of the graphene oxide suspension, which was well dispersed and then heated in a sealed ambient at $85^\circ C$ to induce the polymerization reaction. The polymerized compound including phenolic resin was well washed with ultrapure water, dried in vacuum, and 3D graphene oxide was finally obtained. 3D graphene was obtained by reducing the 3D graphene oxide heated at $1050^\circ C$ for 1 hour under flowing $100\text{ cm}^3/\text{min}$ of Ar/H_2 gas. The reaction scheme was shown in Fig. 1. The 3D graphene oxide and the 3D graphene were characterized with a Raman spectrometer, an X-ray photoemission spectrometer (XPS), and a scanning electron microscopy (SEM).

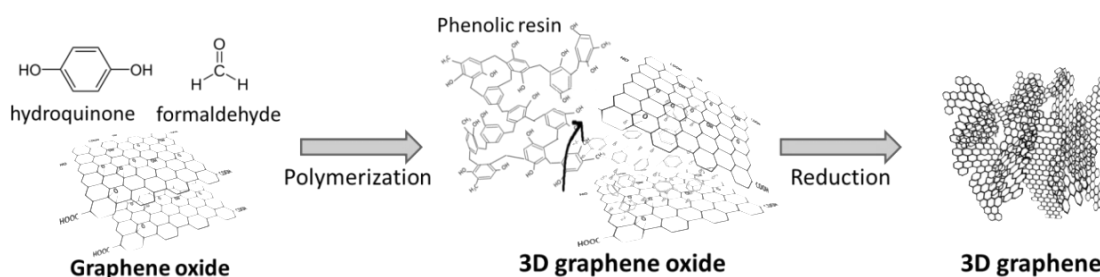


Figure 1 Reaction scheme to synthesize 3D graphene oxide and 3D graphene.

VOCs sensing

Fig.2 illustrates a sensing system of VOCs with 3D graphene oxide and 3D graphene. In the flow system, 4.0 L/min of N_2 gas was used as a carrier gas, and the VOCs such as acetone or 1-butanol were used as VOC markers for a tumor. To control the concentrations of VOCs, the temperature of VOCs was controlled by using ethanol and dry ice or water and ice. The flow rate of VOCs was adjusted with a mass flow controller. In the detection chamber, the concentrations of VOCs were measured with a VOC monitor (photo ionization detection sensor). The 3D graphene oxide or 3D graphene with $10\text{ mm} \times 7\text{ mm} \times 2\text{ mm}$ or $10\text{ mm} \times 2.5\text{ mm} \times 1\text{ mm}$ was mounted in glass plate, of which both sides were pasted and fixed with Ag paste as electrodes. The electrical current response at the fixed voltage of 1.0 V for different VOC concentration was *in situ* measured at room temperature.

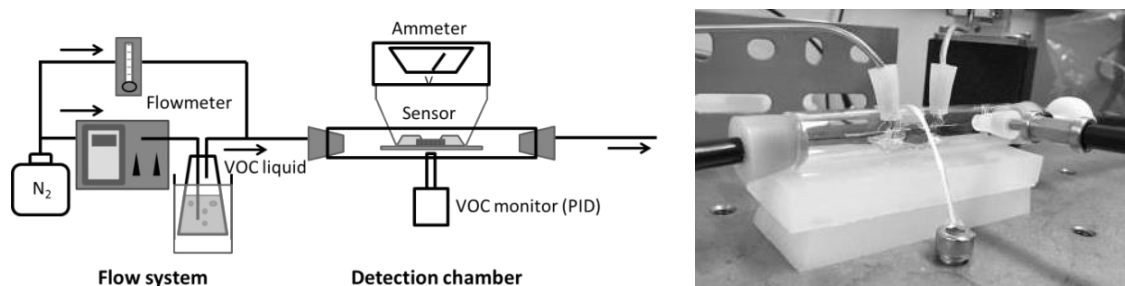


Figure 2 The schematic illustration of sensing system for VOCs (left), and photo of detection chamber (right).

DISCUSSION

Characteristics of 3D graphene oxide and 3D graphene

The microstructure of 3D graphene oxide was obtained as the following mechanism. In graphene oxide suspension, the sheets layered parallel were dispersed, in which the distance between interlayers was larger than that in graphite. Phenolic resins polymerized with hydroquinone and formaldehyde were invaded into the interlayers and fixed graphene oxide sheets randomly. Fig. 3 shows the exteriors and inner structures of 3D graphene oxide and 3D graphene. Both materials had a black color and did not shrink during the polymerization and reduction process. Thus, both 3D materials had a similar micro-structure. It was easily cut with a knife blade. Both 3D materials had a layer-by-layer disordered structure with large pores at 10 μm in diameter.

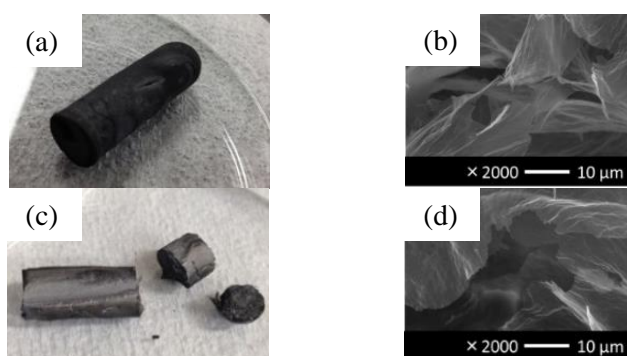


Figure 3 Exteriors and inner structure of (a), (b) 3D graphene oxide and (c), (d) 3D graphene.

Fig. 4 and Fig. 5 illustrate Raman and XPS spectra of 3D graphene oxide and 3D graphene. Raman spectra showed the D, G and 2D bands, indicating a six-membered carbon ring structure and a decrease of oxygen-containing functional groups after reduction. These results were also confirmed by XPS spectra of C_{1s} and O_{1s} ; the intensities of C-O peak at 285.9 eV, C=O peak at 287.1 eV and COOH peak at 288.6 eV were apparently decreased, and the O_{1s} peak at 532 eV was slightly detected after reduction. Electrical conductivity of 3D graphene oxide and 3D graphene devices were approximately 1.0×10^{-2} S/cm and 1.0 S/cm, indicating the reduction increase the conductivity due to the decrease of oxygen-containing functional groups.

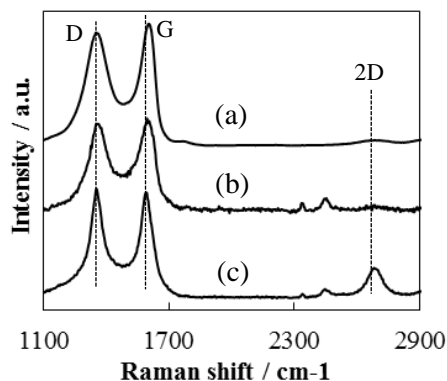


Figure 4 Raman spectra of (a) graphene oxide, (b) 3D graphene oxide, and (c) 3D graphene.

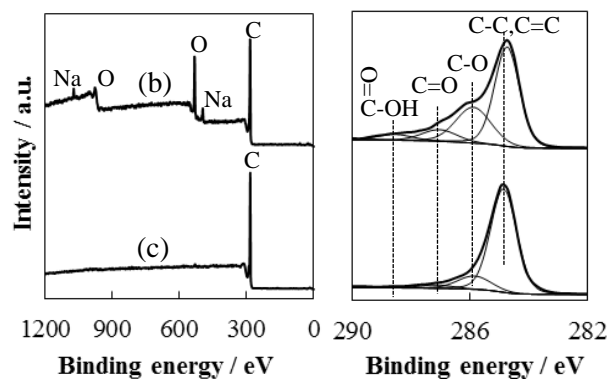


Figure 5 XPS spectra of (b) 3D graphene oxide, and (c) 3D graphene; left side is wide spectra and right side is narrow spectra.

VOC Sensing using 3D graphene device

Fig. 6 shows the current response for adsorption of acetone (300-1000 ppm) and 1-butanol (8-20 ppm) on 3D graphene device. The current responses were not varied under flowing N₂ gas and were correlated with the VOC concentrations, however 3D graphene device responded at high acetone concentration over 300 ppm and with limited sensitivity for the change of concentrations of 1-butanol. It is worth to note that the adsorption of acetone resulted in a decreasing current, but the adsorption of 1-butanol resulted in increased current.

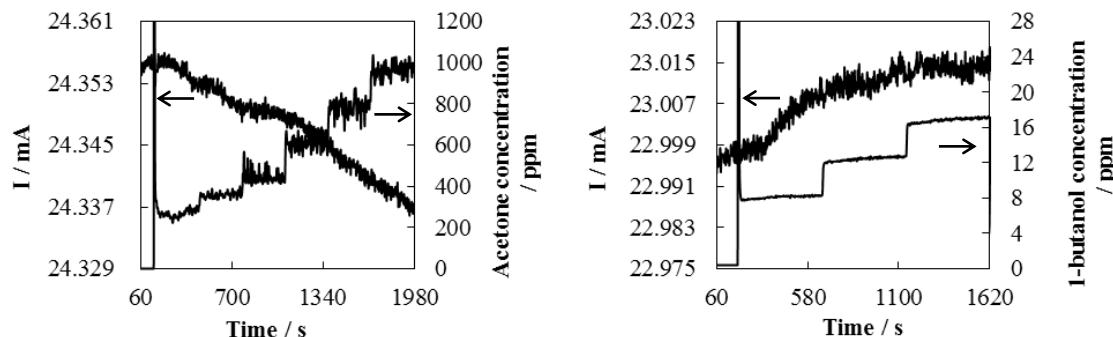


Figure 6 Current responses for adsorption of acetone and 1-butanol on 3D graphene device.

VOC Sensing using 3D graphene oxide device

The 3D graphene oxide device was employed for the detection of VOCs at low concentrations. Interestingly, the baseline of current responses was varied under flow of N₂ gas and increased with increasing time. The variation of baseline was due to desorption of water molecules. The current changes of 3D graphene oxide for the adsorption of VOCs were much sensitive compared with those of 3D graphene, meaning that the lower concentration of VOCs gradually changed the current values. However, it was still difficult to detect the low changes in concentration based upon current change. The baseline for flowing only N₂ gas was thus fitted by the following equations, of which the *a*, *b* and *intercept* values were determined with a least-squares method. The baselines of current values for 1000 s were measured 4 times for the same 3D graphene oxide device, and then the VOCs were flowed in the chamber. The intercept value changed at starting time of the detection, and thus the *a*, *b* and *intercept* value were variable for the individual 3D graphene oxide devices.

$$I = a \times \ln\left(\frac{t}{b} + 1\right) + \text{intercept}$$

Fig. 7 shows an example of baseline for 3D graphene oxide device under flow of N₂ gas. The *a*, *b* and *intercept* values were calculated to be 0.0106, 257.8 and 1.325. By determining these values, the differences of current responses and baseline were plotted versus time.

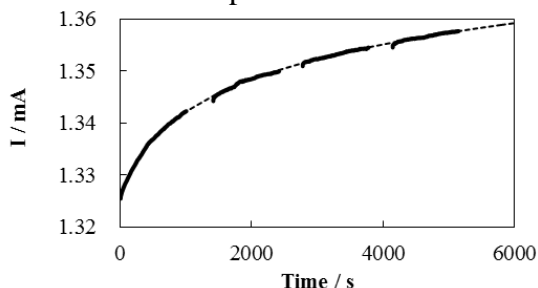


Figure 7 Current variation of the baseline curve under N₂ gas flow for 3D graphene oxide device; the dotted line was the fitted curve, and solid line was the measured curve.

Fig. 8 shows the current responses of 3D graphene oxide device for flowing acetone and 1-butanol at different concentrations. The concentrations were much lower than those for 3D graphene device, and the tendency of current responses was similar to those of 3D graphene; the adsorption of acetone increased the current values, and that of 1-butanol decreased the current values. To understand the baseline current variation, step-wise curves reflecting current changes were clearly observed. The difference in the detection limit for VOCs on 3D graphene oxide device versus 3D graphene device appears to be dependent on the existence of the surface oxygen-containing functional group such as hydroxyl group and carboxyl group on 3D graphene oxide device. It was estimated that detection limit was approximately 5 ppm for acetone. VOCs with high polarity were easily adsorbed on 3D graphene oxide surfaces, since the oxygen-containing functional group strongly interacted with VOCs. The reproducible uses of the sensors should be furthermore investigated; the VOC gases cannot desorb completely from the nano-structure of 3D materials with flowing N_2 gas.

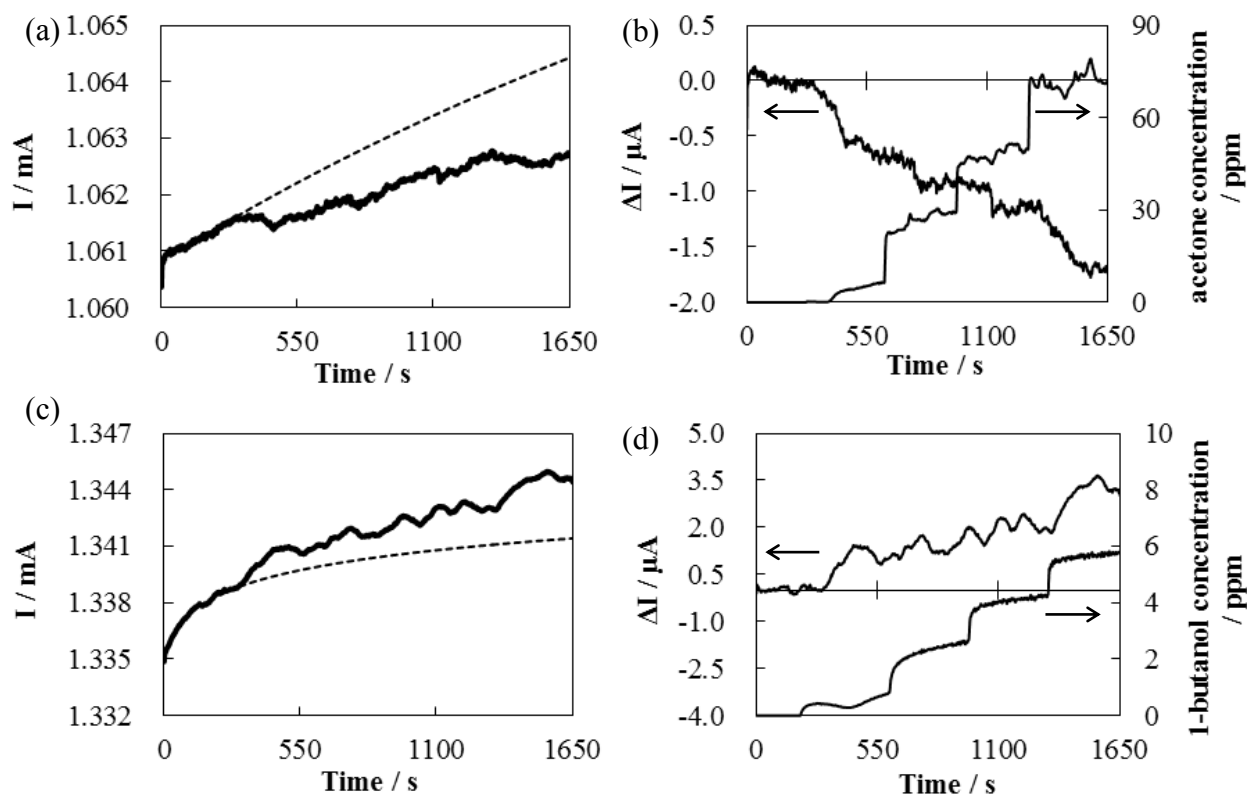


Figure 8 Current responses of 3D graphene oxide device for acetone and 1-butanol at different concentrations; (a), (b) shows the result of acetone, and (c), (d) shows the result of 1-butanol. The differences of current responses and baselines (dotted line) are shown in (b) and (d).

The differences in the current responses were postulated as follows. The acetone and water serve as an electron-withdrawing molecule, and 1-butanol function as an electron-donating molecule to the surfaces. Thus, desorption of water made the current value rise; however adsorption of acetone made it fall but that of 1-butanol made it increase. The results of VOC adsorption on the surface, indicate that both 3D graphene and 3D graphene oxide have potential applications for VOC gas sensing.

CONCLUSIONS

In this study, 3D graphene oxide and 3D graphene devices were successfully fabricated and VOC gas sensing was demonstrated. While the 3D graphene device responded to high VOC concentrations, the 3D graphene oxide device responded not only to high VOC concentrations but also to low concentrations. VOCs with polarity were easily adsorbed on 3D graphene oxide surfaces, since the polar oxygen-containing functional group strongly interacted with the adsorbed VOCs.

REFERENCES

1. K.S. Novoselov, V.I. Falko, L. Colombo, P.R. Gellert, M.G. Schwab, K. Kim, *Nature*, **490**, 192-200 (2012).
2. S.S. Varghese, S. Lonkar, K.K. Singh, S. Swaminathan, *Sensors and Actuators B218*, 160-183 (2015).
3. G.H. Lu, L.E. Ocola, J.H. Chen, *Nanotechnology*, **20**, 445502-4455011 (2009).
4. F. Schedin, A.K. Geim, S.V. Morozov, E.W. Hill, P. Blake, M.I. Katsnelson, K.S. Novoselov, *Nat. Mater.*, **6**, 652-655 (2007).
5. S. Chen, W. Cai, D. Chen, Y. Ren, X. Li, Y. Zhu, J. Kang, R.S. Ruoff., *New J. Phys.*, **12**, 125011 (2010).
6. Y. Ito, Y. Tanabe, H.J. Qiu, K. Sugawara, S. Heguri, N.H. Tu, K. KimHuynh, T. Fujita, T. Takahashi, K. Tanigaki, M. Chen., *Angew. Chem. Int. Ed.*, **53**, 4822-4826 (2014).
7. Z. Chen, W. Ren, L. Gao, B. Liu, S. Pei, H.M. Cheng, *Nat. Mater.*, **10**, 424-428 (2011).
8. Z.M. Wang, K. Hoshino, M. Xue, H. Kanoh, K. Ooi, *Chem. Commun.*, 1696-1697 (2002).
9. M.A. Worsley, T.Y. Olson, J.R.I. Lee, T.M. Willey, M.H. Nielsen, S.K. Roberts, P.J. Pauzauskie, J. Biener, J.H. Satcher, T.F. Baumann., *J. Phy. Chem. Lett.*, **2**, 921-925 (2011).
10. V.H. Luan, J.S. Chung, E.J. Kim, S.H. Hur, *Chem. Eng. J.*, **246**, 64-70 (2014).
11. H. Wang, K. Sun, F. Tao, D.J. Stacchiola, Y.H. Hu. *Angew. Chem. Int. Ed.*, **52**, 9210-9214 (2013).
12. Y.J. Yun, W.G. Hong, N.J. Choi, H.J. Park, S.E. Moon, B.H. Kim, K.B. Song, Y. Jund, H.K. Lee., *Nanoscale*, **1**, 6511-6514 (2014).
13. X. Liua, J. Sunb, X. Zhang., *Sensors Actuators B Chem.*, **211**, 220-226 (2015).
14. J. Huang, S. Kumar, N. Abbassi-Ghadi, P. Španě, D. Smith, G.B. Hanna, *Anal. Chem.*, **85**, 3409-3416 (2013).
15. G. Songa, T. Qina, H. Liua, G.B. Xub, Y.Y. Pana, F.X. Xionga, K.S. Gua, G.P. Suna, Z.D. Chen, *Lung Cancer*, **67**, 227-231 (2010).
16. C. Pei, H. Sun, Z. Zhu, W. Liang, J. An, Q. Zhang, A. Li., *RSC Adv.*, **4**, 14042 (2014).